Deep-Sea Research Part I 136 (2018) 84–90

Contents lists available at ScienceDirect

Deep-Sea Research Part I

journal homepage: www.elsevier.com/locate/dsri

Intraseasonal flow and its impact on the chlorophyll-a concentration in the Sunda Strait and its vicinity

Tengfei Xu[a,b], Shujiang Li[a,b], Faisal Hamzah[c,d], Agus Setiawan[e], R. Dwi Susanto[f,g], Guojiao Cao[a,b], Zexun Wei[a,b,*]

[a] First Institute of Oceanography, State Oceanic Administration, Qingdao 266061, PR China
[b] Laboratory for Regional Oceanography and Numerical Modeling, Qingdao National Laboratory for Marine Science and Technology, Qingdao 266237, PR China
[c] State Key Laboratory of Marine Environmental Science, Xiamen University, Xiamen 361005, PR China
[d] Institute for Marine Research and Observation, Ministry of Marine Affairs and Fisheries, Bali 82251, Indonesia
[e] Research and Development Center for Marine and Coastal Resources, Agency for Marine and Fisheries Research and Development, Ministry of Marine Affairs and Fisheries, Jakarta 14430, Indonesia
[f] Department of Atmospheric and Oceanic Science, University of Maryland, College Park, MD 20742, USA
[g] Faculty of Earth Sciences and Technology, Bandung Institute of Technology, Bandung 40116, Indonesia

ARTICLE INFO

Keywords:
Sunda Strait
Intraseasonal variability
Kelvin waves
Chlorophyll-a
Remote sensing

ABSTRACT

Sunda Strait is the outflow strait of the South China Sea branch of the Pacific to Indian Ocean Throughflow. The annual mean volume transport through the Sunda Strait is around 0.25 Sv from the Java Sea to the eastern Indian Ocean, only 2.5% of the IndonesianThroughflow, and thus has been ignored by previous investigations. However, the Nutrient concentrations in the Sunda Strait and its vicinity are found highly related to the water transport through the Sunda Strait. Particularly, our observation shows significant intraseasonal variability (ISV) of currents at period around 25–45 days in the Sunda Strait. Both remote and local wind forcing contribute to the ISVs in the Sunda Strait. The intraseasonal oscillation of sea surface wind in the central Indian Ocean drives upwelling/downwelling equatorial Kelvin waves to propagate along the equator and subsequently along the Sumatra-Java coasts, resulting in negative/positive sea level anomalies in the south of the Sunda Strait. The local intraseasonal sea surface wind anomalies also tend to induce negative/positive sea level anomalies in the south of the Sunda Strait by offshore/onshore Ekman transport while there are upwelling/downwelling events. The ensuring sea level gradient associated with the sea level anomalies in the south of the Sunda Strait induces intraseasonal outflow (from Indian Ocean to Java Sea) and inflow (from Java Sea to Indian Ocean) through the strait. Analyses also show that the chlorophyll-a concentrations in the south of the Sunda Strait are lower/higher during the inflow/outflow period of the ISV events in March through May. The mechanism attributes to both the nutrient-rich water transported by the intraseasonal flow in the Sunda Strait and by the upwelling and Ekman transport driven by the local sea surface wind anomalies.

1. Introduction

The Sunda Strait locates between the Sumatra and Java Islands (Fig. 1). It connects the Java Sea to the Indian Ocean. The strait stretches in a northeast-southwest orientation, and looks like a funnel with minimum width of 24 km at its northeastern end and maximum width of 110 km at southwestern. The bottom topography in the Sunda Strait slopes to the northeast, that is, deeper in the southwest with maximum water depth over 1000 m, whereas less than 40 m in the northeast. The Sunda Strait is much narrower and shallower than other outflow straits of throughflow from the Pacific to the Indian Ocean, i.e. the Lombok, Ombai Straits and the Timor Passage. As a result, it allows neither large amount of water transport nor significant Kelvin wave penetration into the Sunda Strait, thus have been ignored for decades in the Pacific to Indian Ocean Throughflow and/or regional physical oceanography literatures, as compared with the Lombok, Ombai Straits and the Timor Passage. Nevertheless, given the fact that there are distinguished water properties between the two sides of the Sunda Strait (Fig. 1 in Setiawan et al., 2015), even small water exchange via the strait is able to influence the water mass at each side dramatically, resulting in re-distribution of temperature, salinity as well as chlorophyll and nutrient concentration, which is suggested to affect the spatial variations of

* Corresponding author.
E-mail address: weizx@fio.org.cn (Z. Wei).

https://doi.org/10.1016/j.dsr.2018.04.003
Received 8 August 2017; Received in revised form 16 March 2018; Accepted 9 April 2018
Available online 12 April 2018

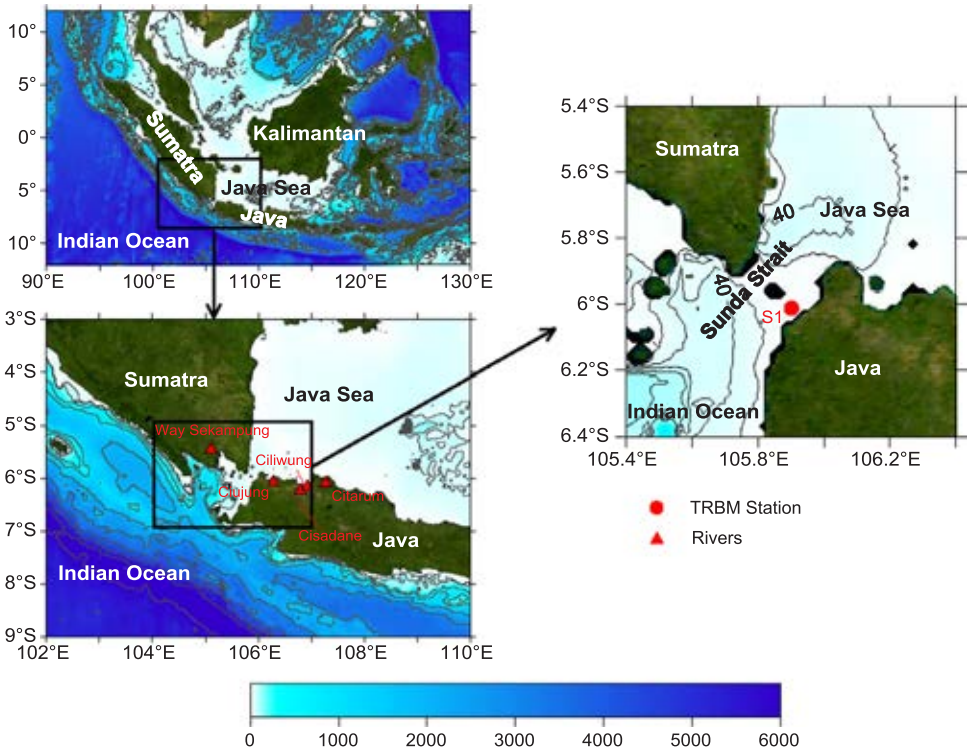

Fig. 1. Maps of the investigation area including bottom topography. The Trawl Resistant Bottom Mount (TRBM) station is located at S1 (5°54.09'S, 105°57.75'E, water depth is 53 m) from February 23, 2010, to September 25, 2011.

phytoplankton community in the Sunda shelf directly (Ke et al., 2014).

So far, there are few investigations conducted to reveal the water exchange and its influences on the regional marine environment and related dynamics in the Sunda Strait. In the NAGA Report, Wyrtki (1961) suggests the water exchange is normally towards the Indian Ocean in the Sunda Strait and is strongly related to the surface gradient of the sea level through the strait, showing the maxima velocity in August and a second peak in December/January. According to Wyrtki (1961), the transport through the Sunda Strait is estimated to be smaller than 0.5 Sv (1 Sv = $10^6 m^3/s$) due to its small cross section. This estimation is confirmed by numerical simulations, which suggest a transport of 0.3 or 0.2 Sv towards the Indian Ocean forced by monthly or 6-hourly winds, respectively (Wannasingha et al., 2003). Other numerical simulations show larger transport with 0.48 Sv (minimum) in December and 0.72 Sv (maximum) in August/September (Putri, 2005). Although these investigations have suggested consistent water transport from the Java Sea to the Indian Ocean throughout the year, there is still large uncertainty about the transport, since no direct measurement has been conducted yet. Observations in the Sunda Strait and its surrounding seas often rely on high resolution image of satellite data and/or cruise survey of hydrological factors, which show that there are three types of water masses around the Sunda Strait (Hendiarti et al., 2002). Hendiarti et al. (2002) also suggests that the Java Sea water with higher chlorophyll-a concentration flows into the Indian Ocean through the Sunda Strait during the Southeast monsoon season, which then influence the biological aspects, such as marine living resources and fisheries around the Sunda Strait (Hendiarti et al., 2004, 2005). Recently, Ke et al. (2014) suggests significant effects of different surface current patterns on the distribution of phytoplankton community around the Sunda Strait based on in situ observations of two cruises in April-May 2010 and 2011, respectively. Since the two cruises are during the monsoon transition season with only one month interval, this variability may attributes to intraseasonal variability (ISV) rather than on other time scale.

Previous studies have suggested that the ISV along the Lesser Sunda Strait is induced by the propagation of intraseasonal Kelvin waves that derived from the equatorial Indian Ocean (Qiu et al., 1999; Wijffels and Meyers, 2004; Iskandar et al., 2005, 2006; Schiller et al., 2010; Chen et al., 2015). These Kelvin waves are able to penetrate into the Indonesian Seas through the Lombok and Ombai Strait, and to reach the Makassar Strait and the Banda Sea, affecting the water transport by altering the vertical structure of the along-strait velocity across the strait (Syamsudin et al., 2004; Sprintall et al., 2009; Drushka et al., 2010; Gordon et al., 2010; Pujiana et al., 2013; Iskandar et al., 2014). Meanwhile, the Madden-Julian Oscillation (MJO) induces intraseasonal variability of sea surface salinity (SSS) and barrier layer thickness through wind stress-forced oceanic dynamical processes and precipitation in the equatorial central and eastern Indian Ocean, which in turn to influence the stratification, resulting in different response of sea surface temperature (Drushka et al., 2014; Guan et al., 2014; Li et al., 2015). The Sunda Strait is the first gap that lies on the pathway of the intraseasonal Kelvin waves along the southwest coast of the Sumatra and Java Islands. Based on initial observation of high resolution velocity profile at the Sunda Strait, Susanto et al. (2016) suggests ISV of the along-strait flow in the Sunda Strait, which can reverse the direction of the seasonal flow during the monsoon transition season from April to May. However, whether the intraseasonal flow is related to the coastally trapped Kelvin waves and how it impacts on the chlorophyll-a concentration thus to affect the fish distribution and abundance, have not been revealed. These two questions will be discussed based on both in situ and satellite observations. The datasets used in this study are described in Section 2. Section 3 explains the dynamics related to the ISV in Sunda Strait. The influences of the intraseasonal flow on the chlorophyll-a concentration in the Sunda Strait and its vicinity are shown in Section 4. Discussions and conclusions are summarized in Section 5.

2. Data and method

Full depth current profiles are observed by Acoustic Doppler

Current Profiler (ADCP) on board of Trawl Resistant Bottom Mount (TRBM), which are supported by "The South China Sea – Indonesian Seas Transport/Exchange (SITE) and Impact on Seasonal Fish Migration" program that conducted jointly by scientists from China, Indonesia, and the United States since 2006 (Fang et al., 2010; Susanto et al., 2010). The TRBM is equipped with an upward-looking, 300 kHz, self-contained ADCP, of which the bin size and sampling intervals are set to 2 m and 20 min, respectively. Sea level data is the Version 5.0 of gridded Sea Level Anomaly (SLA) product produced by Segment Sol multi-missions dALTimetrie d'orbitographie et de localisation precise/Data Unification and Altimeter Combination System (SSALTO/DUACS) and distributed by the AVISO, with support from the CNES (http://www.aviso.altimetry.fr/duacs/). The dataset is daily with a resolution of 0.25° × 0.25°, available from October 1992 to the present (Ducet et al., 2000). The daily sea surface wind fields is obtained from the version 2.0 of the Cross Calibrated Multi-Plantform (CCMP) with a horizontal resolution of 0.25° × 0.25° and time interval of 6 h, provided by the National Aeronautics and Space Administration (NASA) since 2009 (Atlas et al., 2011). The chlorophyll-a concentrations around the Sunda Strait are obtained from the Moderate Resolution Imaging Spectroradiometer (MODIS)/Aqua Level-3 product of surface chlorophyll-a concentration (Hu et al., 2012). The product is mapped on a horizontal resolution about 4.6 km, and covers the period from May 2002 to the present. The sea surface temperature data are obtained from the Advanced Very High Resolution Radiometer (AVHRR) with period from 1981 to the present on a 0.25° × 0.25° grid (Casey et al., 2010). The precipitation data are the monthly Tropical Rainfall Measuring Mission (TRMM) Multi-Satellite Precipitation Analysis (TRMM-3B43) with a horizontal resolution of 0.25° × 0.25° from 1998 to the present (Kummerow et al., 1998; Huffman et al., 2007). The water discharge records are provided by the Research and Development Center for Water Resources, Ministry of Public Works and Housing, Indonesia covers period 2011–2013. The data records were taken from five rivers observation namely Cisadane, Ciliwung, Citarum, Ciujung and Way Sekampung which is disembogued to Java Sea.

Morlet wavelet is adopted as the mother wavelet in the wavelet analysis. The 95% confidence level for the wavelet analysis is calculated based on red noise background spectrum with autoregressive lag 1 correlation of 0.72 (Torrence and Compo, 1998). In order to illustrate the eastward propagation of the ISV in relation to the intraseasonal atmospheric forcing, regression maps are achieved by linearly regressing 20–90-day band-passed sea surface wind anomalies and SLA onto the 20–90-day band-passed vertically averaged along-strait velicity in the Sunda Strait. The significance levels of the regressions are calculated based on the Student's *t*-test.

3. ISVs in Sunda Strait

The time series of wind and flow vectors in the Sunda Strait are shown in Fig. 2. The flow in the shallow Sunda Strait is dominated by the Ekman flow in general, showing the flow direction point to the left side of the wind direction during most of the observation period, with outflow (from the Java Sea to the Indian Ocean) during the southeastward monsoon season and inflow (from the Indian Ocean to the Java Sea) during the northwestward monsoon season. The flow shows similar directions at different depth in the Sunda Strait, suggesting domination of barotropic currents in the strait. Furthermore, the Sunda Strait flow is subjected to ISV, showing reversal of the direction during the monsoon transition season from March to May.

The ISV of the Sunda Strait flow is revealed by power spectra of zonal, meridional and along-strait velocity at different depths at Station S1, which shows similar distribution of power spectra, with typical periods around 25–45 days at all depths (Fig. 3). The along-strait velocity is calculated as

$$w = u\cos\theta + v\sin\theta,\ \theta = 48°$$

Fig. 2. Time series of daily sea surface wind and flow vector in the Sunda Strait (Station S1). Upward and downward vectors indicate northward and southward flows, respectively.

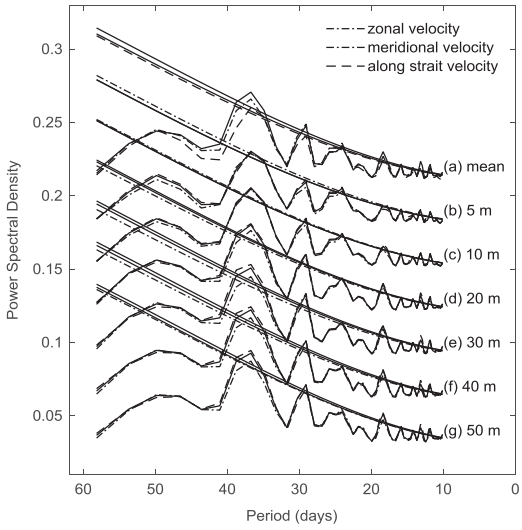

Fig. 3. Power Spectra of the zonal, meridinonal and along strait velocity at different depths. The smooth curves indicate the 95% confidence level.

where u and v are the zonal and meridional velocity, respectively, and θ is the direction of section S1 referenced to true north. For simplicity, we use the vertically averaged velocity for further analyses here after.

The seasonal variability of the Sunda Strait throughflow is evidenced by the seasonal reversal of its direction, i.e. inflow during boreal winter and outflow during summer (Fig. 4a). In addition, strong intraseasonal events of the Sunda Strait throughflow occur during the monsoon transition season, with the maximum vertically averaged velocity reaching 75 cm/s, which may reduce or even reverse the direction of the seasonal mean velocity (Susanto et al., 2016). The standard deviations of the 20–90-day band-passed and 30-day low-passed vertically averaged along-strait velocity in the Sunda Strait are 26.02 and 40.89 cm/s, respectively, suggesting significant intraseasonal variability of the Sunda Strait throughflow, in comparison with the seasonal cycle. Wavelet analysis of the vertically averaged along-strait velocity is shown in Fig. 4b–c. The results show intraseasonal signals occur in May

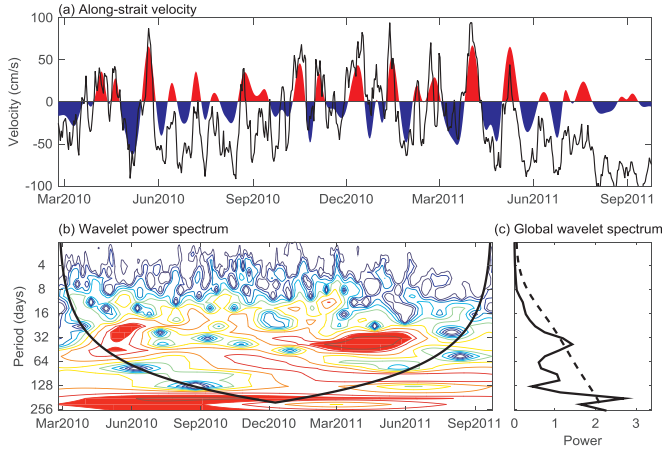

Fig. 4. (a) Raw (solid line) and 20–90 days band-passed (shaded) time series of the vertically averaged along-strait velocity, and its (b) wavelet power spectrum and (c) global wavelet spectrum.

of 2010 and March to May of 2011, with the typical period at around 25–45 days, in agreement with the power spectral analysis.

The 20–90-day band-passed sea surface wind anomalies and SLA are regressed onto the intraseasonal along-strait flow with the later lagged by 15–0 days (Fig. 5). The results show that there are westerly wind anomalies and positive SLA in the equatorial Indian Ocean when the Sunda Strait throughflow lags by 15 days, suggesting downwelling Kelvin waves excited by westerlies with 15 days leading the $+v'$ ISV events (defined as the along-strait velocity are positive and beyond one standard deviation, and vice versus for the $-v'$ ISV events) (Fig. 5a). The westerlies persist and extend to the east in the following days, accompanied by the eastward propagation of positive SLA induced by the downwelling Kelvin waves (Fig. 5b–d). It takes around 9 days for the Kelvin waves to travel from the central equatorial Indian Ocean to the west coast of the Sumatra Island, implying a propagation speed at 2.97–3.57 m/s. The equatorial Kelvin waves are trapped along the eastern boundary and then propagate northwestward and southeastward along the southwestern coast of Sumatra and Java, respectively (Fig. 5e–f). Of the southeastward branch, it takes about 2 days to reach and pass by the Sunda Strait, suggesting a phase speed of ~3.13 m/s for the coastal Kelvin waves (Fig. 5e). Meanwhile, the equatorial Kelvin waves are reflected by the eastern boundary as symmetric Rossby waves to propagate westward off the equatorial (Chen et al., 2017), which are also evidenced by the westward extension of significant positive regression coeffcients along 5°N in the west of Sumatra Island. The regression coefficients of the SLA along the southwest coast of Sumatra and Java are as large as 0.7 at zero time lag, above the 95% confidence level, suggesting coherent mechanism accounting for the ISVs of SLA in the south of Sunda Strait and along the coast, which in turn involve in driving the ISVs of the Sunda Strait throughflow (Fig. 5f).

The regression map shows no significant relation of the Sunda Strait throughflow to either the sea surface wind anomalies or SLA in the Java Sea and the Sunda Strait from 15 to 9 days lag (Fig. 5a–c). During the time lag of 0–6 days, there are weak westerlies around the Sunda Strait in the Java Sea, which force offshore Ekman transport, resulting in negative SLA in the Java Sea (Fig. 5d–f). The SLA pressure gradient along the Sunda Strait, therefore, is established by both the positive SLA induced by the propagation of downwelling Kelvin waves, and negative SLA that driven by the offshore Ekman transport, in the south and north of the strait, respectively. This pressure gradient is the direct forcing responsible for the intraseasonal outflow from the Indian Ocean to the Java Sea through the Sunda Strait. The regression coefficients in the Java Sea are much weaker, suggesting that the SLA variability in the north of the strait probably plays minor role in forcing the ISVs in the Sunda Strait. The processes are similar for the intraseasonal upwelling events, but with negative SLA in the south of the Sunda Strait, resulting in sea level gradient towards the Indian Ocean, thus forces net inflow through the Sunda Strait.

4. Influences of ISVs on the chlorophyll-a concentration

The chlorophyll-a concentrations surrounding the Sunda Strait are dominated by the river discharge and the coastal upwelling, in the Java Sea and along the southern coast of Sumatra and Java, respectively (Asanuma et al., 2003; Hendiarti et al., 2004; Susanto et al., 2006; Iskandar et al., 2009). There are larger/smaller amount of total river discharge of five main rivers that disembogued to the western Java Sea during rainy/dry season (Fig. 6a). Correspondingly, the chlorophyll-a concentrations in the Java Sea side of the Sunda Strait are generally

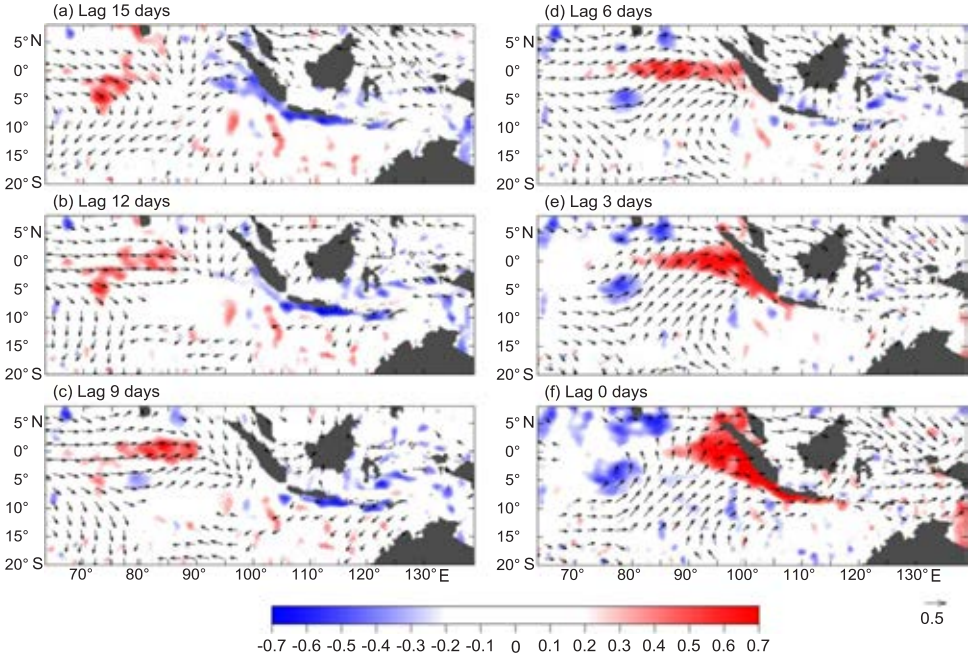

Fig. 5. Lagged regression maps of the 20–90-day band-passed sea surface wind anomalies (vector, m/s) and SLA (shaded, cm) onto the 20–90-day band-passed vertically averaged along strait velocity. (a)–(f) indicate the along strait velocity lags by 15 to 0 day at 3 days interval. The 0 day time lag refers to the regression of two time series at same period.

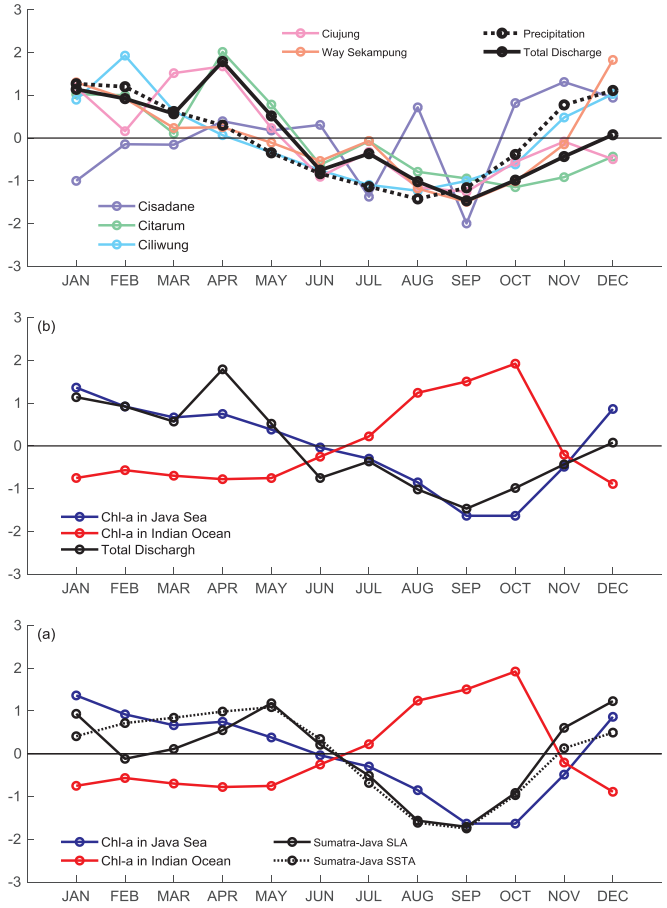

Fig. 6. (a) Climatological precipitation (area averaged over [103.125–108.125°E, 7.875–3.375°S]) and freshwater discharge from five rivers empty to the western Java Sea over periods 2011–2013. (b) Chlorophyll-a concentrations averaged over the western Java Sea [105.875–108.125°E, 5.875–4.125°S] and along the southern coast of Sumatra-Java Islands [101.979–105.854°E, 7.354–3.979°S , and 105.896–108.146°E , 8.688–6.979°S] and total freshwater discharge of the five rivers to the western Java Sea. (c) Chlorophyll-a concentrations averaged over the western Java Sea and Indian Ocean and SLA and SSTA averaged along the southern coast of Sumatra-Java Islands [101.875–105.875°E, 7.375–4.125°S , and 106.125–108.125°E , 8.625–6.875°S]. All of the time series are normalized for inter-comparison.

higher during the rainy season, while large amount of river discharg waters bring more nutrient into the western Java Sea; On the contrary, the chlorophyll-a concentrations in the Indian Ocean side of the Sunda Strait are lower during the rainy season (Fig. 6b), and higher during the southeast monsoon (June to September), while the upwelling that evidenced by lower sea level anomalies and sea surface temperature anomalies (SSTA) along the southwestern coast of Sumatra and Java brings nutrient-rich water from the deeper layer to the surface (Fig. 6c). During the monsoon transition season, remote and local winds force reversal of net water transport in the Sunda Strait at intraseasonal time scale, showing outflow from the Java Sea to the Indian Ocean. Although the total transport through the Sunda Strait is small, these strong ISVs, however, are believed to be important for local marine environment by the frequent water exchange through the strait.

The intraseasonal along-strait flow in the Sunda Strait is generally in phase with the intraseasonal SLA in the south of the Sunda Strait during the observation period (Fig. 7). Therefore, we use the area averaged SLA over [103.125–105.125°E, 6.875–6.125°S] instead of the along-strait velocity to identify the $+v'$/- v' ISV events. The composite analysis of chlorophyll-a concentrations in the Sunda Strait is achieved by averaging the chlorophyll-a concentrations at the peak of each $+v'$/- v' ISV events. The composite analysis is done for each calendar months, respectively. It is worth noting that the chlorophyll-a data are not been band-passed since its time series are not continuous due to cloud coverage. Consequently, besides of the instraseasonal signal, the seasonal and interannual signals of the chlorophyll-a variability may also involve in the analysis. Nevertheless, since the composite analysis is based on the 20–90-day band-passed SLA, the intraseasonal signal of the chlorophyll-a may still significant.

During the monsoon transition season (March to May), positive ISV events transport Indian Ocean water into the Java Sea through the Sunda Strait. Since the chlorophyll-a has no bloom in the absence of the Java coastal upwelling, the chlorophyll-a concentrations are lower in the south of the Java Strait (Fig. 8a–c). On the contrary, composite of chlorophyll-a concentration during negative ISV events from March to May, show high values in the south of the Sunda Strait, suggesting penetration of nutrient-rich water from the Java Sea into the Indian Ocean driven by the intraseasonal southward along-strait flow (Fig. 8d–f). It is worth noting that the sea surface winds play same roles as the intraseasonal along-strait flow for either + v' or -v' events, i.e. favoring lower/higher chlorophyll-a concentrations in the south of the Sunda Strait during ± v' events (Fig. 8). During ± v' events, there are westerlies/easterlies over the Sunda Strait, which tend to force westward/eastward transport of surface water, resulting in more/less eastward extension of sea surface chlorophyll-a from the eastern coast of Sumatra Island. The more/less eastward extension of sea surface chlorophyll-a then contribute to lower/higher chlorophyll-a concentrations of the penetrated water from Java to Indian Ocean. We have not shown the composite chlorophyll-a concentrations in the rest months for two seasons: 1) from June to October, the effect of intraseasonal transport of chlorophyll-a is overwhelmed by that induced by the coastal upwelling along the southern coast of Sumatra and Java; and 2) during boreal winter (December to February), the satellite derived chlorophyll-a is poorly covered due to heavy clouds, leading to large uncertainty for the analysis at intraseasonal time scale.

5. Summary

In this study, we reveal the intraseasonal variability of the Sunda Strait throughflow based on in situ velocity profiles on board of TRBM at station S1 (5°54.09'S, 105°57.75'E). The observation provides a 579-day full-depth measurement of velocity from February 23, 2010, to September 25, 2011. The velocity is projected onto normal and tangential directions along the strait, with the later referred to as along-strait flow. The Sunda Strait throughflow is basically driven by monsoon, which flows towards the Java Sea or the Indian Ocean during the southeast or northwest monsoon seasons, respectively. Besides of the seasonal cycle in association with the monsoon driven circulation, the Sunda Strait throughflow is also subjected to strong intraseasonal variability. The amplitudes of the intraseasonal along-strait velocity can reach to ± 70 cm/s, with a standard deviation of 26.02 cm/s, about 63.6% of its seasonal cycle. These ISVs are strong enough to reverse the direction of the seasonal Sunda Strait throughflow driven by monsoon.

Previous investigations suggest that the ISV of SLA along the Sumatra-Java coasts is dominated by remote forcing from the equatorial Indian Ocean wind stress, with the local wind forcing playing a secondary role (Chen et al., 2015, 2016). The processes proposed by Chen et al., (2015, 2016) are involved in the ISVs in the Sunda Strait. The intraseasonal oscillation of sea surface wind anomalies in the central equatorial Indian Ocean force upwelling/downwelling to propagate eastward as equatorial Kelvin waves, which then be trapped as coastal Kelvin waves to propagate along the Sumatra-Java coasts. While passing by the Sunda Strait, the upwelling/downwelling Kelvin waves induce corresponding negative/positive sea level anomalies in the south of the Sunda Strait, accounting for positive/negative sea level gradient towards the Indian Ocean in the Sunda Strait. Meanwhile,

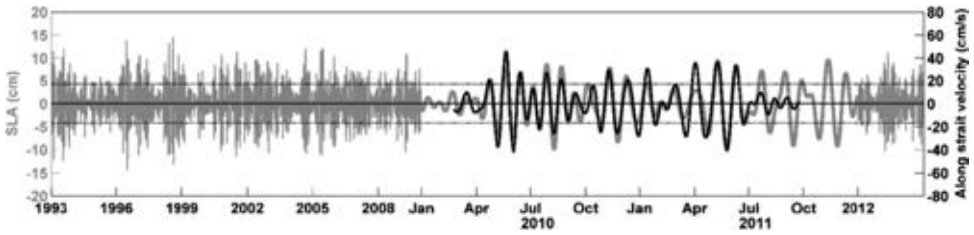

Fig. 7. Time series of the 20–90-day band-passed SLA (gray line) in the south of the Sunda Strait (averaged over [103.125–105.125°E, 6.875–6.125°S]) and the 20–90-day band-passed along-strait velocity (dark line) in the Sunda Strait. Notice that the scale of axis is not uniform in order to compare the detailed phase matching during the SITE periods.

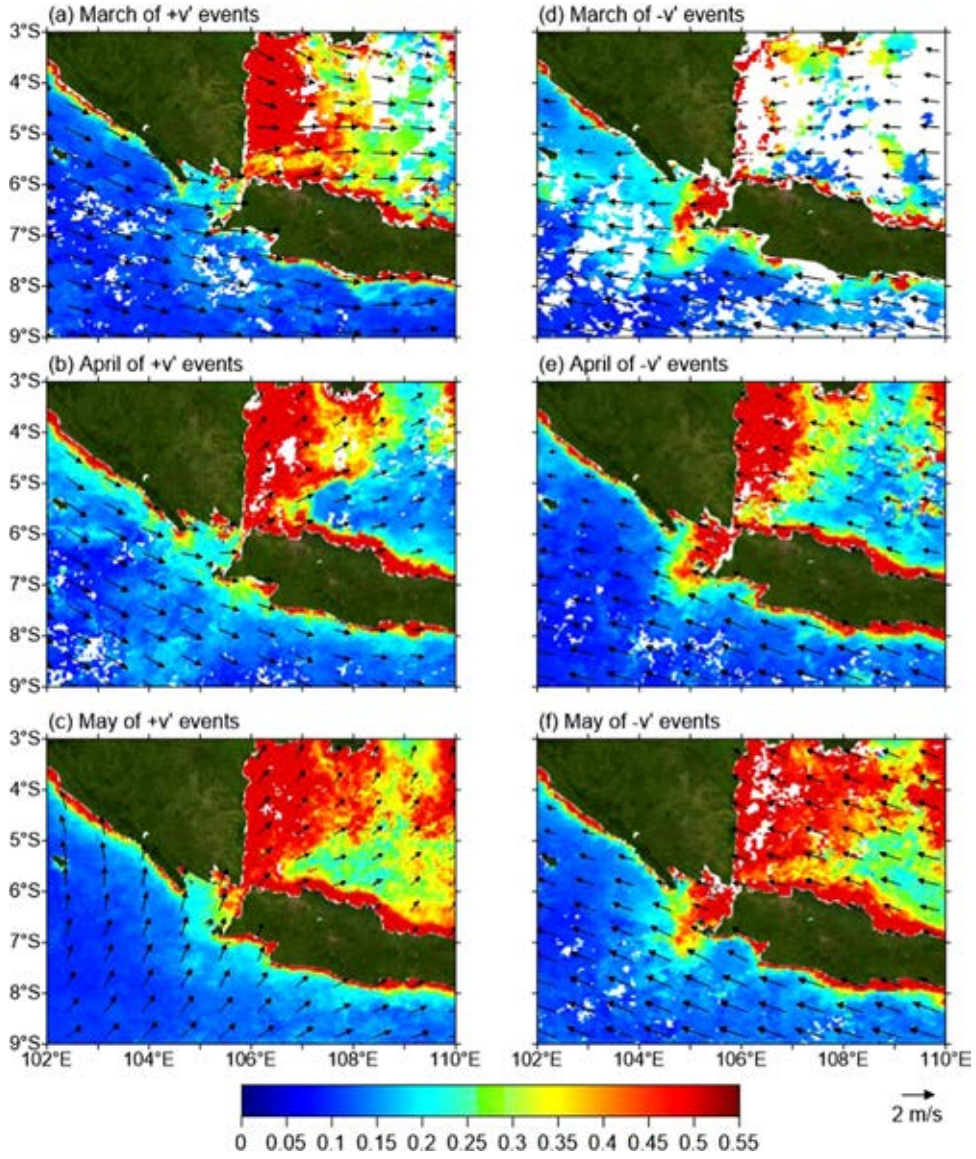

Fig. 8. Composite chlorophyll-a concentrations (unit: mg/m^3) and sea surface winds (unit: m/s) for (a)–(c) positive and (d)–(f) negative ISV events from March through May. The positive and negative ISV events refer to the net inflow (form Indian Ocean to Java Sea) and net outflow (from Java Sea to Indian Ocean) through the Sunda Strait, respectively.

local wind anomalies tend to force offshore/onshore transport along the southern coast of the Sumatra and Java Islands. Consequently, both of the remote and local forcing favor sea level gradient from the Java Sea towards the Indian Ocean to induce net outflow during the intraseasonal upwelling period, whereas from the Indian Ocean towards the Java Sea to induce net inflow during the intraseasonal downwelling period.

The importance of the ISVs in the Sunda Strait lies in the fact that it is capable of inducing notable water exchange through the strait at intraseasonal frequency, thus to influence the ocean hydrological environment in the Sunda Strait and its vicinity. Our analyses show that in March-April-May, when the ISV events are active in the Sunda Strait, the chlorophyll-a concentrations in the south of the Sunda Strait are lower during positive ISV events and higher during negative ISV events. Both the ISVs of the Sunda Strait throughflow and local sea surface wind contribute to the intraseasonal distribution of chlorophyll-a concentrations in the south of the Sunda Strait. This ISVs induced chlorophyll-a concentration variability is potentially important for the estimation of primary productivity in the Sunda Strait and its vicinity.

Acknowledgements

This study is jointly supported by the National Natural Science Foundation of China (Grant Nos. 41506036, 41476025, and 41306031), the SOA Program on Global Change and Air-Sea interactions (GASI-IPOVAI-03 and GASI-IPOVAI-02), the NSFC-Shandong Joint Fund for Marine Science Research Centers (Grant No. U1406405), the China Postdoctoral Science Foundation funded project (Grant No. 2014M561883), and the Postdoctoral Innovation Foundation of Shandong Province (Grant No. 201403019). The U.S. part of the Sunda Strait observation is supported by the Office of Naval Research, USA (Grant No. N00014-08-01-0618). We also appreciate the captain and the crews of the research vessels Baruna Jaya IV, I, and VIII for their skillful operation during the voyages and their cooperation in fieldwork, and we thank all participants in the cruises.

References

Asanuma, I., Matsumoto, K., Okano, H., Kawano, T., Hendiarti, N., Sachoemar, S.I., 2003. Spatial distribution of phytoplankton along the Sunda Islands: the monsoon anomaly in 1998. J. Geophys. Res. 108, 3202. http://dx.doi.org/10.1029/1999JC000139.

Atlas, R., Hoffman, R.N., Ardizzone, J., Leidner, S.M., Jusem, J.C., Smith, D.K., Gombos, D., 2011. A cross-calibrated, multiplatform ocean surface wind velocity product for meteorological and oceanographic applicatons. Bull. Am. Meteor. Soc. 92, 157–174. http://dx.doi.org/10.1175/2010BAMS2946.1.

Casey, K.S., Brandon, T.B., Cornillon, P., Evans, R., 2010. The past, present, and future of the AVHRR pathfinder SST program. In: Barale, V., Gower, J., Alberotanza, L. (Eds.), Oceanography from Space. Springer, Dordrecht. http://dx.doi.org/10.1007/978-90-481-8681-5_16.

Chen, G., Han, W., Li, Y., Wang, D., Shinoda, T., 2015. Intraseasonal variability of upwelling in the equatorial Eastern Indian Ocean. J. Geophys. Res: Oceans 120, 7598–7615. http://dx.doi.org/10.1002/2015JC011223.

Chen, G., Han, W., Li, Y., Wang, D., 2016. Interannual variability of equatorial eastern indian ocean upwelling: local versus remote forcing. J. Phys. Oceanogr. 46, 789–807.

Chen, G., Han, W., Li, Y., Mcphaden, M., Chen, J., Wang, W., Wang, D., 2017. Strong intraseasonal variability of meridional currents near 5°N in the Eastern Indian Ocean: characteristics and causes. J. Phys. Oceanogr. 47, 979–998.

Drushka, K., Sprintall, J., Gille, S.T., Brodjonegoro, I., 2010. Vertical structure of Kelvin waves in the Indonesian Throughflow exit passages. J. Phys. Oceanogr. 40, 1965–1987.

Drushka, K., Sprintall, J., Gille, S.T., 2014. Subseasonal variations in salinity and barrier-layer thickness in the eastern equatorial Indian Ocean. J. Geophys. Res. 119, 805–823. http://dx.doi.org/10.1002/2013JC009422.

Ducet, N., Le Traon, P.Y., Reverdin, G., 2000. Global high resolution mapping of ocean circulation from TOPEX/POSEIDON and ERS-1/2. J. Geophys. Res. 105, 19477–19498.

Fang, G.H., Susanto, R.D., Wirasantosa, S., Qiao, F.L., Supangat, A., Fan, B., Wei, Z.X., Sulistiyo, B., Li, S.J., 2010. Volume, heat and freshwater transports from the South China Sea to Indonesian seas in the boreal winter of 2007–2008. J. Geophys. Res. 115, C12020. http://dx.doi.org/10.1029/2010JC006225.

Gordon, A.L., Sprintall, J., van Aken, H.M., Susanto, R.D., Wijffels, S.E., Molcard, R., Ffield, A., Pranowo, W., Wirasantosa, S., 2010. The Indonesian Throughflow during 2004–2006 as observed by the INSTANT program. Dyn. Atmos. Oceans 50, 115–128.

Guan, B., Lee, T., Halkides, D.J., Waliser, D.E., 2014. Aquarius surface salinity and the Madden-Julian Oscillation: the role of salinity in surface layer density and potential energy. Geophys. Res. Lett. 41, 2858–2869. http://dx.doi.org/10.1002/2014GL059704.

Hendiarti, N., Siegel, H., Ohde, T., Hendiarti, N., Siegel, H., 2002. Distinction of different water masses in and around the Sunda Strait: satellite observations and in-situ measurements. Proc. Porsec. 2002 2, 674–679.

Hendiarti, N., Siegel, H., Ohde, T., 2004. Investigation of different coastal processes in Indonesian waters using SeaWiFS data. Deep-Sea Res. II 51, 85–97.

Hendiarti, N., Suwarso, Aldrian, E., Amri, K., Andiastuti, R., Sachoemar, S., Wahyono, I.B., 2005. Seasonal variation of pelagic fish catch around java. Oceanography 18, 112–123.

Hu, C., Lee, Z., Franz, B.A., 2012. Chlorophyll-a algorithms for oligotrophic oceans: a novel approach based on three-band reflectance difference. J. Geophys. Res. 117, C01011. http://dx.doi.org/10.1029/2011JC007395.

Huffman, G.J., Adler, R.F., Bolvin, D.T., Gu, G., Nelkin, E.J., Bowman, K.P., Hong, Y., Stocker, E.F., Wolff, D.B., 2007. The TRMM Multisatellite Precipitation Analysis (TMPA): quasi-global, multiyear, combined-sensor precipitation estimates at fine scales. J. Hydrometeorol. 8, 38–55.

Iskandar, I., Mardiansyah, W., Masumoto, Y., Yamagata, T., 2005. Intraseasonal Kelvin waves along the southern coast of Sumatra and Java. J. Geophys. Res. 110, C04013. http://dx.doi.org/10.1029/2004JC002508.

Iskandar, I., Tozuka, T., Sasaki, H., Masumoto, Y., Yamagata, T., 2006. Intraseasonal variations of surface and subsurface currents off Java as simulated in a high-resolution ocean general circulation model. J. Geophys. Res. 111, C12015. http://dx.doi.org/10.1029/2006JC003486.

Iskandar, I., Rao, S.A., Tozuka, T., 2009. Chlorophyll-a bloom along the southern coasts of Java and Sumatra during 2006. Int. J. Remote Sens. 30 (3), 663–671.

Iskandar, I., Masumoto, Y., Mizuno, K., Sasaki, H., Affandi, A.K., Setiabudidaya, D., Syamsuddin, F., 2014. Coherent intraseasonal oceanic variations in the eastern equatorial Indian Ocean and in the Lombok and Ombai Straits from observations and a high-resolution OGCM. J. Geophys. Res. 119, 615–630.

Ke, Z., Tan, Y., Ma, Y., Huang, L., Wang, S., 2014. Effects of surface current patterns on spatial variations of phytoplankton community and environmental factors in Sunda shelf. Cont. Shelf Res. 82, 119–127.

Kummerow, C., Barnes, W., Kozu, T., Shiue, J., Simpson, J., 1998. The Tropical Rainfall Measuring Mission (TRMM) sensor package. J. Atmos. Ocean. Technol. 15, 809–817.

Li, Y., Han, W., Lee, T., 2015. Intraseasonal sea surface salinity variability in the equatorial Indo-Pacific Ocean induced by Madden-Julian oscillations. J. Geophys. Res. 120 (3), 2233–2258. http://dx.doi.org/10.1002/2014jc010647.

Pujiana, K., Gordon, A.L., Sprintall, J., 2013. Intraseasonal Kelvin wave in Makassar Strait. J. Geophys. Res. 118, 2023–2034.

Putri, M.R., 2005. Study of Ocean Climate Variability (1959–2002) in the Eastern Indian Ocean, Java Sea and Sunda Strait using the HAMburg Shelf Ocean Model (Dissertation). Univ. Hamburg, pp. 104.

Qiu, B., Mao, M., Kashino, Y., 1999. Intraseasonal variability in the Indo-Pacific Throughflow and the regions surrounding the Indonesian Seas. J. Phys. Oceanogr. 29, 1599–1618.

Schiller, A., Wijffels, S.E., Sprintall, J., Molcard, R., Oke, P.R., 2010. Pathways of intraseasonal variability in the Indonesian Throughflow region. Dyn. Atmos. Oceans 50, 174–200.

Setiawan, R.Y., Mohtadi, M., Southon, J., Groeneveld, J., Steinke, S., Hebbeln, D., 2015. The consequences of opening the Sunda Strait on the hydrography of the eastern tropical Indian Ocean. Paleoceanography 30, 1358–1372.

Sprintall, J., Wijffels, S.E., Molcard, R., Jaya, I., 2009. Direct estimates of the Indonesian Throughflow entering the Indian Ocean: 2004–2006. J. Geophys. Res. 114, C07001. http://dx.doi.org/10.1029/2008JC005257.

Susanto, R.D., Moore II, T.S., Marra, J., 2006. Ocean color variability in the Indonesian Seas during the SeaWiFS era. Geochem. Geophys. Geosyst. 7, Q05021. http://dx.doi.org/10.1029/2005GC001009.

Susanto, R.D., Fang, G.H., Soesilo, I., Zheng, Q.A., Qiao, F.L., Wei, Z.X., Sulistyo, B., 2010. New surveys of a branch of the Indonesian Throughflow. EOS Trans. AGU 91, 261–263.

Susanto, R.D., Wei, Z.X., Adi, T.R., Zheng, Q.A., Fang, G.H., Fan, B., Supangat, A., Agustiadi, T., Li, S.J., Trenggono, M., Setiawan, A., 2016. Oceanography surrounding Krakatau Volcano in the Sunda Strait, Indonesian. Oceanography 29 (2), 264–272.

Syamsudin, F., Kaneko, A., Haidvogel, D.B., 2004. Numerical and observational estimates of Indian Ocean Kelvin wave intrusion into Lombok Strait. Geophys. Res. Lett. 31, L24307. http://dx.doi.org/10.1029/2004GL021227.

Torrence, C., Compo, G.P., 1998. A practical guide to wavelet analysis. Bull. Am. Meteor Soc. 79, 61–78.

Wannasingha, U., Webb, D.J., de Cuevas, B.A., Coward, A.C., 2003. On the Indonesian Throughflow in the OCCAM Model. 〈http://www.noc.soton.ac.uk/JRD/OCCAM/POSTERS/P1_Indonesia.pdf.EGS〉 meeting, Nice.

Wijffels, S.E., Meyers, G., 2004. An intersection of oceanic waveguides: variability in the Indonesian Throughflow region. J. Phys. Oceanogr. 34, 1232–1253.

Wyrtki, K., 1961. Physical Oceanography of Southeast Asian Waters. NAGA Report. 2. Scripps Institution of Oceanography, La Jolla, CA, pp. 195.